 doi:10.20944/preprints202206.0037.v1

Article

Comparison of the mechanical properties of fiber reinforced shotcrete at laboratory and on-site conditions

Ramiro Castellanos Castellón [1], Marcos G. Alberti [2], Jaime C. Gálvez [3,*], J. Vera-Agulló [4], R. Pina-Zapardiel[5]

1 Departamento de Ingeniería Civil: Construcción, E.T.S de Ingenieros de Caminos, Canales y Puertos, Universidad Politécnica de Madrid. C/Profesor Aranguren no 3, 28040, Madrid; ramiro.castellanos@upm.es
2 Departamento de Ingeniería Civil: Construcción, E.T.S de Ingenieros de Caminos, Canales y Puertos, Universidad Politécnica de Madrid. C/Profesor Aranguren no 3, 28040, Madrid; marcos.garcia@upm.es
3 Departamento de Ingeniería Civil: Construcción, E.T.S de Ingenieros de Caminos, Canales y Puertos, Universidad Politécnica de Madrid. C/Profesor Aranguren no 3, 28040, Madrid; jaime.galvez@upm.es
4 ACCIONA Construction S.A., Technological Center, Valportillo II n 8, Madrid 28108, Spain; jose.vera.agullo@acciona.com
5 ACCIONA Construction S.A., Technological Center, Valportillo II n 8, Madrid 28108, Spain; raul.pina.zapardiel@acciona.com

Abstract: Steel fibers (SF) and polyolefin (PF) are widely used for shotcrete, especially in tunnelling. Both SF and PF and have shown to meet the standards in order to reduce or substitute the conventional steel mesh as reinforcement of concrete showing mechanical and productive advantages. This study sought the analysis and assessment of the mechanical properties of fiber reinforced shotcrete, comparing in-situ with laboratory results. This was performed with low and high fiber dosages of SF and PF as well as a combination of them (hybrid mixtures). A total of seven mixtures, two of steel, two of polyolefins, two hybrids and a control mixture were manufactured at laboratory and in situ. By performing tests according to EN 14651 and slabs according to EN 14488-5, it was possible to characterize the residual flexural strengths (f_{Rj}), and energy absorption capacity (E_{25mm}) in slabs. In addition, a fracture surface analysis was performed, and the orientation factor was obtained. This allowed the authors to quantify the loss of residual strength on site and correlate it with the fiber content and positioning. Moreover, some relationships between beam and slab tests were found, allowing to correlate the most relevant type of tests in the field of fiber reinforced concrete.

Keywords: Fracture energy (G_F), energy absorption capacity (E_{25mm}), residual flexural strength(f_{Rj}), fibers

1. Introduction

Shotcrete is widely used in different construction processes, most of the classical examples are structural repair and rehabilitation, construction of tunnels and soil slopes or rock stabilization. To prevent cracking of the shotcrete layer, steel mesh is usually placed before the spraying process. The process of placing these meshes is very laborious and time-consuming. Also, the presence of this mesh produces a "shadow" effect, causing the formation of hollow or empty zones due to the difficulty of penetration of the shotcrete behind the mesh. As an alternative to the use of these mesh, the incorporation of fibers avoids the "shadow" effect, and improves crack resistance, strengthening the sprayed concrete layer. In fact, in many projects the use of steel mesh has been replaced by the use of fiber-reinforced shotcrete (FRS) [1].

Due to the severe load conditions and deformations during the span life of the tunnel, structural, steel or polyolefin macro-fibers are adopted. They improve the toughness and energy absorption capacity of the hardened concrete, reducing deformability [2]. In addition, high-ductility fibers provide to shotcrete homogeneous fiber reinforcement and higher adhesion to the application surface [3].

Preprints (www.preprints.org) | NOT PEER-REVIEWED | Posted: 3 June 2022 doi:10.20944/preprints202206.0037.v1

Other advantages of using fibers are: ease of use and adaptation to the geometry of the ground; increased efficiency and speed for primary stabilization. The fiber reinforced shotcrete (FRS) application process offers a substantial improvement in safety over methods such as the use of mesh [4,5], particularly in primary stabilization. Time lost in mines and tunnels has been shown to decrease significantly compared with meshing since FRS was adopted as a support method [6]. Finally, fibers offer better performance and corrosion resistance than steel reinforcement [7,8], and synthetic macro-fibers offer a very high degree of crack degradation resistance [9-11]. This has lead the way for the use of FRS as a permanent soil support [12].

Considering the benefits of steel and polymeric fibers, several authors have shown [13,14] that hybrid mixtures, incorporating two or three different types of fibers in a cementitious system, result in a composite with higher engineering performance and better mechanical properties. Studies carried out in the field of sprayed concrete with hybrid fibers have shown an improvement and performance in the energy absorption capacity for tests on beams and slabs [15,1,16].

This paper describes the methodology for the evaluation of wet mix shotcrete reinforced with steel fibers, polyolefin and hybrid combinations. A comparative analysis of the mechanical properties obtained in the laboratory and on site was carried out. Properties such as flexural residual tensile strength (f_{Rj}), fracture energy (G_F), and energy absorption capacity (E_{25mm}) in plates were characterized. Fracture surface analysis was also performed to identify and obtain the differences between the effective fiber content in the laboratory and on-site conditions.

2. Experimental campaign

The experimental campaign considered a total of seven mixes based on the type and content of fibres: a control dosage (without fibres), two mixtures with steel fibres (30 and 50kg/m^3 respectively), two mixtures with polyolefin fibers (7 and 10 kg/m^3), and two mixtures with hybrid combinations of 25+5 kg/m^3 and 20+7kg/m^3, being the first number the content of steel fibers, and the second the content of polyolefin fibers. These dosages are based on the amounts of fibers proposed by various researchers in experimental campaigns [16-17].

The objective of analysis the behaviour of these mixtures was to study the influence of the type of the fibres, firstly with steel fibers and polyolefin separately, and secondly the potential synergy of both type of fibres working together.

(**a**) (**b**)

Figure 1. Experimental campaign on site: (**a**) Placement of molds in the tunnel; (**b**) Revision of molds with shotcrete

The characterization of the residual flexural strength was carried out according to the UNE-EN 14651 standard [18]. The fracture energy of the tested specimens was also

Preprints (www.preprints.org) | NOT PEER-REVIEWED | Posted: 3 June 2022 doi:10.20944/preprints202206.0037.v1

determined. Once these tests were concluded, the analysis of the fracture surface was performed, executing the respective counts to determine the number of effective fibers and to obtain the orientation factor [19,20] in the fractured section. This procedure was carried out for the laboratory and shotcrete beams.

Figure 1 describes the process of obtaining samples on site. The concrete was cast directly on metal forms (for beams) and wooden forms (for slabs), maintaining an angle of 20º with the vertical plane at the time of its elaboration, a requirement specified by UNE-EN 14488-1 [21]. In addition to the study of beams, the energy absorption capacity of the plates was determined for a deflection of 25 mm [22], according to the EN 14488-5 standard

2.1. Materials

The aggregates used were of the siliceous type consisting of 0/4 mm washed sand and 2/8 mm crushed coarse aggregate; the combination of fine aggregate-coarse aggregate selected was 70-30% respectively. This granulometry met the requirements for sprayed concrete according to Annex 9 of the Spanish Structural Code [23]. All the dosages used Portland cement type I 52.5 R of high initial strength. To control the flowability of the mixture, Sika Viscocrete 5970 polycarboxylic superplasticizer was used in dosages of 1.3 to 1.65% by weight of cement to obtain a slump type S5 (26+/-2cm) [23].

The combinations made included steel fibers with hooked ends (Dramix 3D 65/35), and straight embossed polyolefin fibers (Sikaforce 48). The physical and mechanical properties of the fibers used in the present experimental campaign are shown in Table 2.

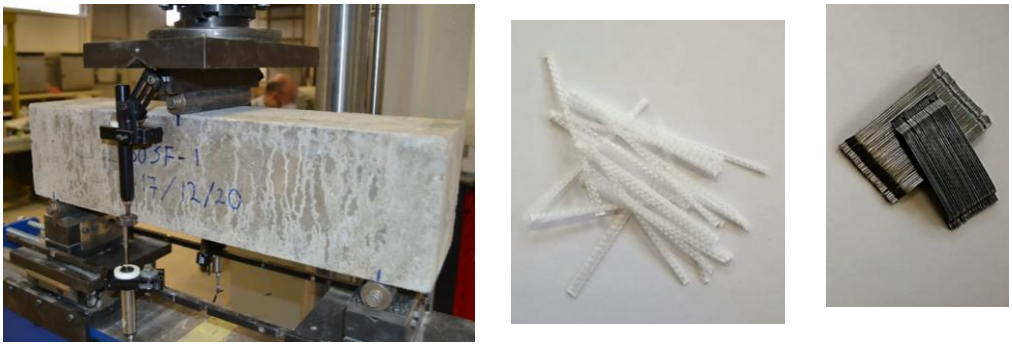

(**a**) (b) (c)

Figure 2. (**a**)Beam prepared for three-point bending test according to EN 14651 standard. Fibers used in the experimental campaign: (**b**) Sikaforce 48; (**c**) Dramix 65/35.

The spraying equipment was a Sika-Putzmeister PM 407 gunite mixer, which used an alkali-free accelerator (Sigunit L-5601) dosed at 4% by weight of the cement. The water/cement ratio for mixtures prepared in the laboratory was 0.45, and 0.48 for the on site mixtures because it was not possible to pump and project a mix for the lower w/c ratio. The dosages of cement, aggregates and fiber content are specified in Table 1.

Preprints (www.preprints.org) | NOT PEER-REVIEWED | Posted: 3 June 2022 doi:10.20944/preprints202206.0037.v1

Table 1. Dosages studied in wet mix fiber reinforced shotcrete

Mix	Shotcrete (Kg/m³)				Amount of fibers (Kg/m³)	
	Cement	Water[1]	Gravel	Sand	SF	PF
Control	440	198	548	1281	-	-
50SF	440	198	548	1281	50	-
30SF	440	198	548	1281	30	-
7PF	440	198	548	1281	-	7
10PF	440	198	548	1281	-	10
25SF5PF	440	198	548	1281	25	5
20SF7PF	440	198	548	1281	20	7

[1] the amount of water in tunnel mixes was 211 liters/m³, w/c = 0.48

Table 2. Physical and mechanical properties of the fibers used in the experimental campaign.

Fiber	Length (mm)	Diameter (mm)	Slender-ness (L_f/de)	Tensile strength (MPa)	Modulus of elasticity (GPa)	Density (gr/cm3)
RC-65/35-BN	35	0.55	63.63	1345	210	7.850
Sikaforce-48	48	0.84	57.14	465	7.5	0.901

2.2. Test procedures

2.2.1. Residual flexural strength

For this analysis, the flexural tensile strength test was performed according to EN 14651:2007+A1 [18], the specimen dimensions were 150x150x600mm, with a free span of 500mm between supports, a notch was made maintaining a ligament in the fracture section of 125±1mm. To measure the vertical displacement, two devices (LVDT) were used on both sides of the beam. The measurement of the notch opening was monitored with an extensometer (CMOD). The specimen setup and test monitoring devices are shown in Fig. 2a. For each dosage, two to three beams were tested. From these tests, average values and curves were obtained to facilitate the analysis process; these data and curves are shown in Table 4 and Figure 6

2.2.2. Fracture surface analysis (Fiber count and orientation factor)

The analysis of the fracture surface was necessary to validate the mechanical behavior of the beams tested in flexural tensile strength. To obtain the number of fibers in the fractured faces, the methodology used by RILEM TC 162-TDF [19] was adopted. The counting process was carried out by dividing the fracture section into 9 equal areas (Fig. 3) without taking into account the notch, this process allowed visualizing the fiber dispersion, if it was homogeneous, or how disturbed it was by the wall effect.

Figure 3. Analysis of the fracture section of specimen 7PF-1 (Shotcrete sample).

As a complement to the counting, the orientation factor (θ) was obtained on the fracture surfaces, which made it possible to compare the actual number of fibers counted with

Preprints (www.preprints.org) | NOT PEER-REVIEWED | Posted: 3 June 2022 doi:10.20944/preprints202206.0037.v1

the theoretical number of fibers according to the dosage performed. In this sense, if the fibers were totally aligned, the number of fibers counted would coincide with the theoretical value, therefore, the proportion θ would be unity. Equations 1 and 2 provide the methodology for calculating the theoretical fibers and the orientation factor in the fractured section.

$$\#\ theoretical\ fibers = \frac{A \cdot V_f}{A_f} \quad (1)$$

A: fracture surface
V_f: volumetric fraction
A_f: cross-sectional area of fiber

$$\theta = \frac{\#\ counted\ fibers}{\#\ theoretical\ fibers} \quad (2)$$

2.2.3. Energy absorption in plates

This test was carried out according to EN 14488-5 standard on fiber-reinforced plates, which met the theoretical dimensions of 600x600x100mm3.. The specimens were tested under displacement control . The load was applied by means of a rigid steel block of square section of 100x100mm² and 20 mm of thickness,. In addition, a sheet of wood of dimensions 100x100mm² and 20 mm of thickness was placed to ensure the correct transmission of the applied load to the concrete surface. On both sides of the rigid block, two bars were extended for the placement of extensometers to measure the relative vertical displacement between the center of the plate and the support surface of the metal frame on which the specimen rests. The support frame complied with the standard dimensions, consisting of a square metal frame with internal dimensions of 500x500mm², with a thickness of 20mm and a height of 80mm to allow the necessary vertical displacement at the center of the specimen during the test. Figure 4 shows the test setup.

Figure 4. 10PF plate test assembled according to EN 14488-5 [22].

According to EN 14488-5, the energy absorption capacity of the specimen is the the area under the load-deformation curve, for a deflection of 25 mm at the center of the plate, being able to classify this energy absorption in three classes. The classification is presented in Table 3.

Preprints (www.preprints.org) | NOT PEER-REVIEWED | Posted: 3 June 2022 doi:10.20944/preprints202206.0037.v1

Table 3. Energy absorption requirements according to EFNARC.

Toughness class	Energy Absorption for deflection up to 25 mm (J)
a	500
b	700
c	1000

3. Experimental results and discussion

3.1. Residual flexural strengths

The characteristic values of f_{R1}, f_{R2}, f_{R3} and f_{R4} of all the specimens tested are presented in Table 4, which will be used for the analysis of the following sections. In addition, Table 5 shows the results of the fiber counts, which allowed to interpret the mechanical behavior described below.

3.1.1. Steel fibers

Figures 6a and 6b compare the behaviour of the specimens cast in the laboratory (*L*) and sprayed in situ (*G*), both for concrete with steel fiber (30 and 50 kg/m^3) . As can be seen in Figures 6a and 6b, for crack openings (CMOD) up to 2 mm, the specimens cast in laboratory showed much higher residual strengths. Comparing the average values of f_{R1}, the results obtained in the laboratory specimens were 46% and 73% higher than the gunned specimens, for the 50SF and 30SF combinations, respectively. For crack openings greater than 2 mm, and taking into account the average value of f_{R3}, the results showed that the laboratory specimens were 11% higher than their shotcrete counterparts in both concrete mixes with steel fibres. This difference in residual strength capacity was according to the content of fibers in the fracture surface of the laboratory and shotcrete specimens. The average values of fiber count in the fracture section were 11% and 23% higher for the laboratory specimens than for in situ specimens for the 30SF and 50SF mixtures, respectively.

In addition, the residual strength corresponding to the proportionality limit f_{LOP}, both in laboratory and in situ specimens with higher fiber content (50SF), performed better than 30SF. For example, the 50SF laboratory specimens increased the proportionality limit strength (f_{LOP}) by 23%; in the case of the shotcrete specimens, an increase of 13% was reported in favor of the 50 kg/m^3 dosage formulation. This behavior has already been reported by several authors [16,24,17].

3.1.2. Polyolefin fibers

The only dosage that had a similar behavior in the laboratory and on site was 7PF (Fig. 6c). It is worth noting that the average number of fibers counted in the shotcrete sample was 168, exceeding the 132 fibres counted in the fracture section of the laboratory specimen. Despite the difference in number, all these specimens presented similar mechanical behavior. Although the shotcrete beams had a higher count of fibres in the fracture section, most of their fibers failed by sliding (136) and a lower number by breaking (33), while in the laboratory specimen there was a higher number of broken fibers (53) in proportion to their slipped fibers (80).

The difference in f_{R1} values (Figure 6c and 6d), comparing the laboratory and shotcrete beams, was 5 to 20% higher in favor of the laboratory beams, for 7PF and 10PF dosages, respectively. In addition, the value of f_{R3} was 23% higher for the laboratory specimen with 10 kg of polyolefin (10PF), while the gunned specimen with 7 kg of fiber reported a slightly higher value (2% higher) than the laboratory specimen.

Both polyolefin combinations reported a higher number of slipped fibers in their field specimens compared with the laboratory specimens. Moreover, the laboratory specimens showed a higher number of broken fibers in relation to the shotcrete specimens. This behavior can be attributed to a better anchorage of the fiber to the matrix in the laboratory specimens, due to a better orientation angle compared with the fibers in the shotcrete specimens.

Preprints (www.preprints.org) | NOT PEER-REVIEWED | Posted: 3 June 2022 doi:10.20944/preprints202206.0037.v1

Table 4. Residual flexural strength average curve values.

Nº	Beam	f_{LOP}	CMOD (0.5mm)							
		f_{LOP} (MPa)	f_{R1} (Mpa)	%f_{LOP}	f_{R2} (Mpa)	%f_{LOP}	f_{R3} (Mpa)	%f_{LOP}	f_{R4} (Mpa)	%f_{LOP}
1	Control	4.62	0.43	**9%**	-	-	-	-	-	-
2	30SF (L)	4.98	4.25	**85%**	2.88	**58%**	1.83	**37%**	1.40	28%
3	50SF (L)	6.11	5.51	**90%**	4.70	**77%**	3.10	**51%**	2.36	39%
4	7PF (L)	4.49	1.91	**43%**	2.11	**47%**	2.33	**52%**	2.44	54%
5	10PF (L)	4.02	2.49	**62%**	2.99	**74%**	3.27	**81%**	3.30	82%
6	25SF5PF (L)	4.58	4.01	**88%**	3.92	**86%**	3.08	**67%**	2.70	59%
7	20SF7PF (L)	3.85	3.58	**93%**	3.55	**92%**	3.47	**90%**	3.30	86%
8	30SF (G)	4.20	2.46	**58%**	1.98	**47%**	1.64	**39%**	1.33	32%
9	50SF (G)	4.76	3.77	**79%**	3.45	**73%**	2.81	**59%**	2.46	52%
10	7PF (G)	4.63	1.81	**39%**	2.25	**49%**	2.37	**51%**	2.37	51%
11	10PF (G)	4.08	2.08	**51%**	2.52	**62%**	2.65	**65%**	2.59	63%
12	25SF5PF (G)	4.79	3.19	**67%**	3.13	**65%**	2.85	**59%**	2.61	54%
13	20SF7PF (G)	5.18	2.88	**56%**	2.98	**58%**	2.80	**54%**	2.55	49%

3.1.3. Hybrid mixes

For the hybrid mixes, the laboratory 25SF5PF combination performed better than the results of the shotcrete beams, and this behavior was maintained until the crack opening reached approximately 4 mm (see Fig. 6e). For CMOD larger than 4mm, the load carrying capacity was approximately the same.

Performing the analysis of f_{R1} values for the shotcrete and laboratory beams, both hybrid mixes (20SF7PF and 25SF5PF) were outperformed by their laboratory counterparts by 25%. For CMOD values of 2.5 mm (f_{R3}), the increases in residual flexural strength were 10 and 24% in the laboratory specimens, corresponding to the 25SF5PF and 20SF7PF mixes, respectively.

The specimens cast in laboratory showed higher values of fiber count in the fractured section than specimens sprayed on site. For example, for the 20SF7PF combination, 218 fibers were counted in the laboratory specimen, *vs.* 187 in the on site specimen section. Similarly, the 25SF5PF combination reported 212 fibers in the laboratory specimen *vs.* 181 in the on site specimen. This increase in fiber content in the laboratory specimens resulted in better performance than the shotcrete specimens for initial deflections (Fig. 6e) and throughout the whole test (Fig. 6f).

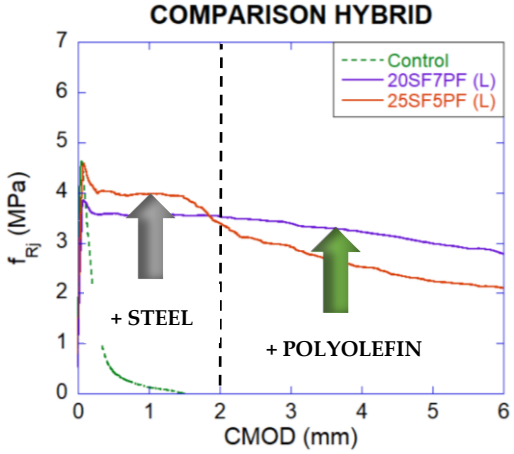

Figure 5. Average results of the three point bending tests of the laboratory specimens with hybrid mixtures of fibres.

Finally, Fig. 5 shows the average curves of the three point bending tests of the laboratory specimens with hybrid mixtures of fibres, where the synergy and effect of a higher or lower content of steel or polyolefin fibers was evident. The combination with higher

Preprints (www.preprints.org) | NOT PEER-REVIEWED | Posted: 3 June 2022 doi:10.20944/preprints202206.0037.v1

content of steel fibres (25SF5PF), once the peak load (f_{LOP}) was exceeded, led to higher residual strength up to 2 mm of crack opening, followed by a controlled decrease in load. The combination with higher content of polyolefin fibres (20SF7PF) led to lower initial loading capacity up to 2 mm CMOD, but was able to obtain much higher remaining strength than the combination 25SF5PF. The higher content of steel fibres led to higher loadings for initial crack openings, while the higher content of polyolefin fibres showed the better performance for larger crack openings.

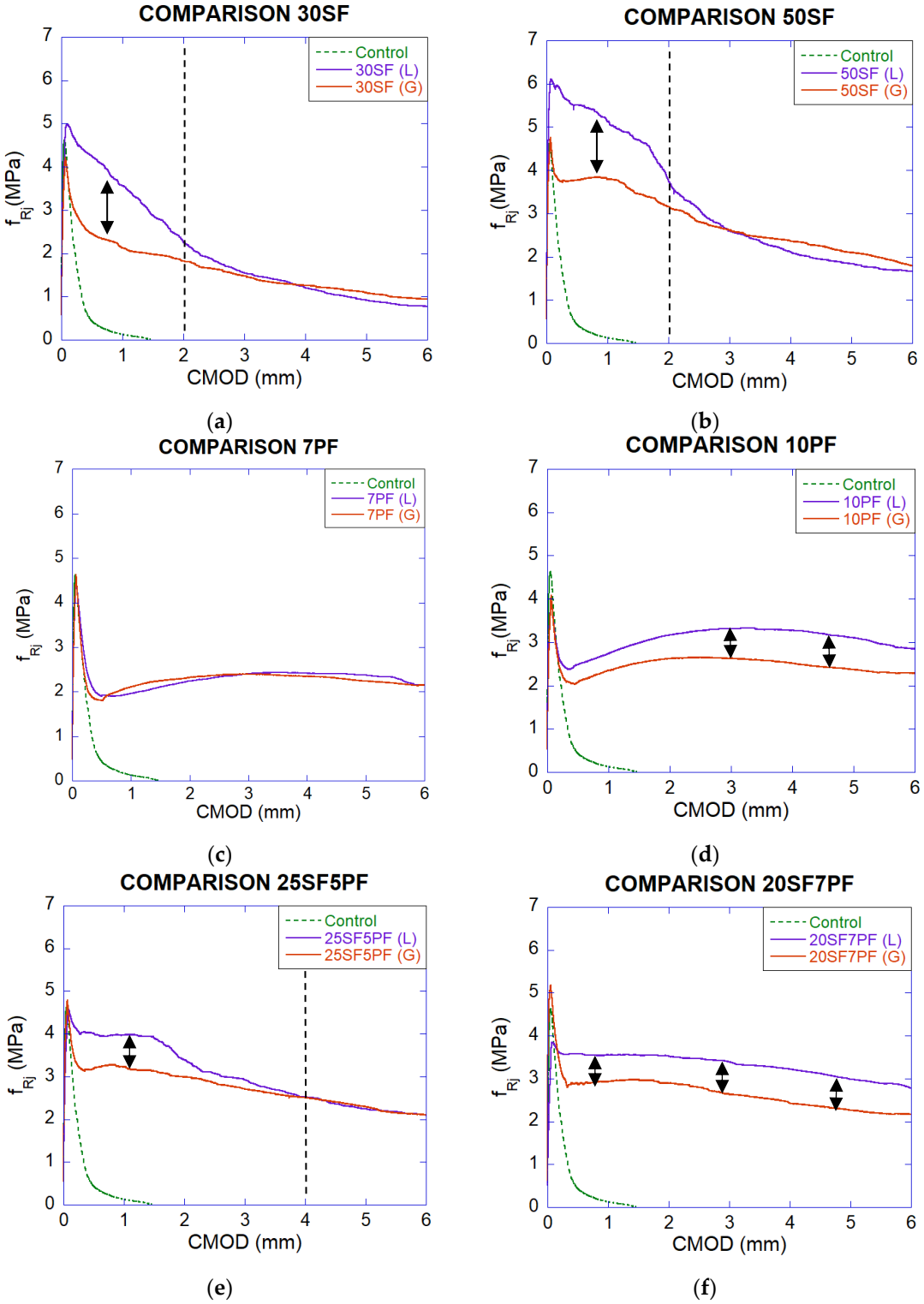

Figure 6. Curvas f_{Rj}-CMOD en laboratorio y obra: (**a**) 30SF; (**b**) 50SF; (**c**) 7PF; (**d**) 10PF; (**e**) 25SF5PF; (**f**) 20SF7PF. Notes: (L)Laboratory beams;(G) Shotcreted or on site beams

Preprints (www.preprints.org) | NOT PEER-REVIEWED | Posted: 3 June 2022 doi:10.20944/preprints202206.0037.v1

Table 5. Fiber counts in the fracture section, site and laboratory specimens.

Beam	(Broken)	Average Broken	(Slipped)	Average slipped	# Total count	Average Total	# Total theoretical	Orientation factor (θ)
C1-1	-	-	-	-				
C1-2	-	-	-	-	-	-	-	-
30SF-1 (L)	-	-	114	-	114	121	315	0.36
30SF-2 (L)	-	-	127	-	127	(0.08)	316	0.40
30SF-1 (G)	-	-	130	-	130	109	311	0.42
30SF-2 (G)	-	-	88	-	88	(0.27)	304	0.29
50SF-1 (L)	-	-	255	-	255	221	524	0.49
50SF-2 (L)	-	-	186	-	186	(0.22)	535	0.35
50SF-1 (G)	-	-	197	-	197	180	506	0.39
50SF-2 (G)	-	-	162	-	162	(0.14)	509	0.32
7PF-1 (L)	46	**53**	86	**80**	132	132	283	0.47
7PF-2 (L)	59	(0.17)	73	(0.11)	132	(0.00)	281	0.47
7PF-1 (G)	27	**33**	132	**136**	159	168	267	0.60
7PF-2 (G)	38	(0.24)	139	(0.04)	177	(0.08)	271	0.65
10PF-1 (L)	65	**66**	118	**109**	183	175	384	0.48
10PF-2 (L)	67	(0.02)	100	(0.12)	167	(0.06)	390	0.43
10PF-1 (G)	37	**36**	140	**148**	177	184	379	0.47
10PF-2 (G)	34	(0.06)	156	(0.08)	190	(0.05)	379	0.50
25SF5PF-1 (L)	48	**41**	162	**171**	210	212	449	0.47
25SF5PF-2 (L)	33	(0.19)	180	(0.06)	213	(0.01)	454	0.47
25SF5PF-1 (G)	22	**20**	155	**161**	177	181	403	0.44
25SF5PF-2 (G)	17	(0.18)	167	(0.05)	184	(0.03)	406	0.45
20SF7PF-1 (L)	48	**41**	187	**177**	235	218	483	0.49
20SF7PF-2 (L)	42	(0.18)	174	(0.05)	216	(0.07)	483	0.45
20SF7PF-3 (L)	33		171		204		477	0.43
20SF7PF-1 (G)	21	**19**	136	**168**	157	**187**	471	**0.33**
20SF7PF-2 (G)	17	(0.15)	200	(0.27)	217	(0.23)	467	0.46

3.2. Analysis of fracture section and assesment of orientation factor

The values of the orientation factor, the analysis of the fractured section, and the failure mode of the fibers allowed are useful for comparing the differences of mechanical behavior between the laboratory and on site cast specimens. The values of orientation factor are presented in Fig. 7 and described below.

- **Steel fibers**

As it can be seen in Figure 8a and 8b, for the 50SF mix, the amount and difference of distribution of steel fibers in the fracture section of the specimens cast on site (G) vs. laboratory (L) was significant. The fracture section of the specimen cast in laboratory shows better homogeneity and distribution of fibers than the fractured section of the shotcrete specimen. The latter shows wall effect and accumulation of fibers in the perpendicular plane (bottom of the form) to the shotcrete application. The orientation factor of the fibres in the fracture section of the on-site specimens is lower than the one of the laboratory steel specimens.. This difference being more significant for the 50SF dosage, θ values of 0.42 and 0.35 were reported for the laboratory and on site beams, respectively.

This behavior could be attributed to the percentage of rebound and impact caused in the spraying process, due to the stiffness of the steel fiber, which has a reduced adhesion capacity to the concrete matrix in the fresh state, compared with fiber of polymeric origin during shotcrete [25-27]. In the present experimental campaign, the higher the content of steel fibers in the spraying process led to the greater difference of the orientation factor

Preprints (www.preprints.org) | NOT PEER-REVIEWED | Posted: 3 June 2022 doi:10.20944/preprints202206.0037.v1

between the laboratory and on site specimen values. These differences of the orientation factor and the homogeneity of the fibre distribution in the fracture section are the main cause that explain the better performance of residual flexural tensile strengths of the laboratory specimens in comparison with the on site sprayed specimens.

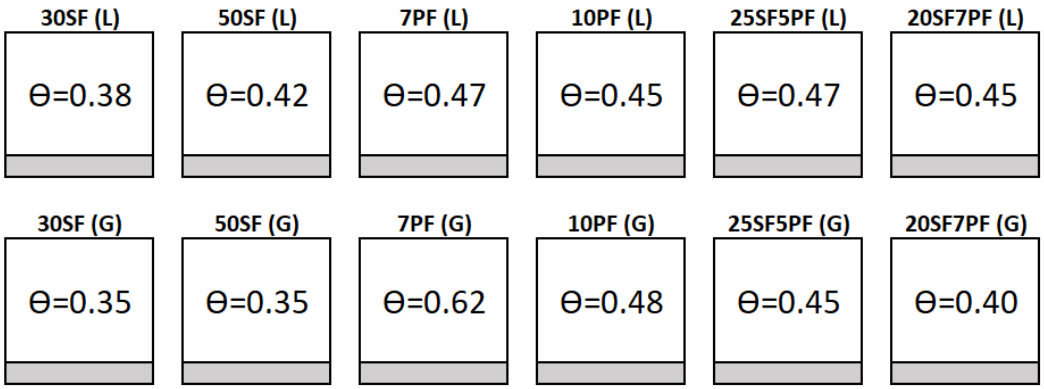

Figure 7. Average orientation factor of the laboratory (L) and shotcrete (G) specimens obtained from the fibres count in the fracture section.

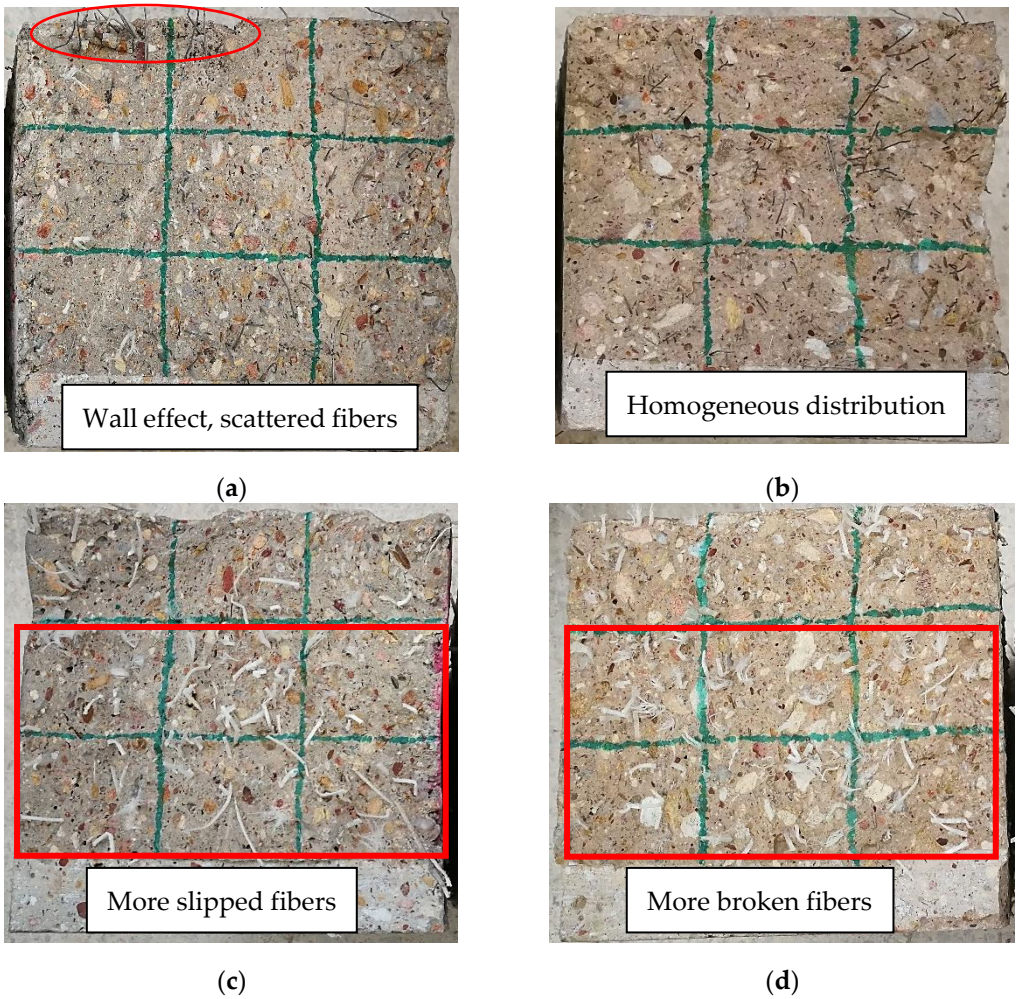

Figure 8. Fracture section analysis: (**a**) 50SF(G); (**b**) 50SF(L); (**c**) 10PF(G); (**d**) 10PF(L).

- **Polyolefin fibers**

The specimens with polyolefin fibres sprayed in reported higher orientation factors than the ones performed with steel fibres This is attributed to the fact that polyolefin fiber in shotcrete applications, having lower stiffness than steel one, is able to better adhesion

Preprints (www.preprints.org) | NOT PEER-REVIEWED | Posted: 3 June 2022 doi:10.20944/preprints202206.0037.v1

on the impact surface, dissipating kinetic energy and ensuring better adhesion to the concrete matrix in the fresh state [25]. The 7PF combination showed a significant difference, with θ values of 0.62 and 0.47, in the site and laboratory specimens, respectively. The fracture surface of the laboratory specimens showed higher value of the broken fibres than the fracture surface of the on site specimens. In addition, the number of fibres that failed by slippage is higher in the fracture surface of the on site specimens. These differences may be explained taking into account the difference between casting procedure of the laboratory specimens in comparison with in situ specimens.

Figures 8c and 8d show the difference in failure mechanism in the 10PF specimens for on site sprayed and laboratory cast specimens, being higher the number of broken fibers in laboratory specimens. Table 5 shows the values of the fibres counting From what was mentioned and seen in Fig.6c we can say that a lower content of broken fibers could equate to the work of several slipped fibers.

- **Hybrid mixes of fibres**

The orientation factor of the fracture surface of the sprayed concrete, with hybrid mixes of fibres, in situ was lower than the corresponding to the specimens cast in laboratory in both cases (25SF5PF, 20SF7PF), as Figure 7 shows. In addition, the number of broken fibres in the fracture surface was lower for the on site specimens, and the number of slipped fibres larger, in comparison with the specimens cast in laboratory

3.3. Fracture energy

3.3.1. Comparison between laboratory vs on site beams

Initially, the difference in fracture energy between the laboratory and field specimens was evaluated by means of the ratio $G_{F(Laboratory)}/G_{F(shotcrete)}$, the values are expressed as a percentage. Deformations of 2.5, 5 and 10 mm were considered for this analysis. According to Figure 9 it can be appreciated a typical behavior, in four of the six dosages studied, as the deflection increased, the difference in fracture energy between the laboratory and site specimens decreased. For example, for the 30SF and 50SF combinations, the difference in fracture energy for a 2.5 mm deflection was 49% and 31 % respectively. While for a 10 mm deflection the magnitudes were reduced to 13% and 6%. In addition, beams 7PF and 25SF5PF led to same fracture energy for in situ fand laboratory specimens for a deflection of 10 mm. Only the combinations 10PF and 20SF7PF exceeded the fracture values of their field specimens by 29 %and 22% for the highest strain (10 mm).

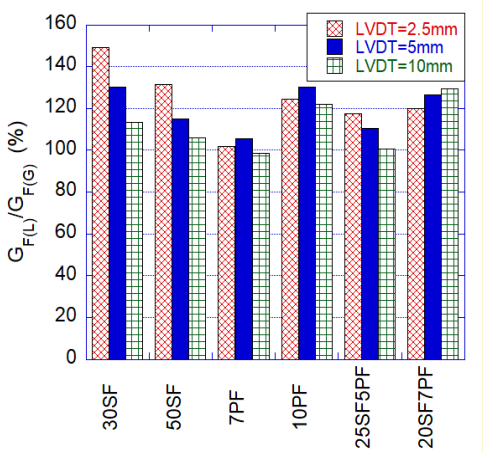

Figure 9. Fracture energy ratio between laboratory and on site specimens.

Considering 2.5 and 5 mm deflections, the difference between laboratory andon site fracture energies was in the range of 49% to 2% and 30% to 5%, respectively. Being evident the reduction and approximation of these values in all the mixtures with the increase of the deformation.

Preprints (www.preprints.org) | NOT PEER-REVIEWED | Posted: 3 June 2022 doi:10.20944/preprints202206.0037.v1

3.3.2. Comparison between Steel and hybrid mixes

The description and analysis of the tested beams are accompanied by the letters (L) or (G) representing the laboratory and in situ specimens, respectively. This designation for the beams will be used in this and later sections.

For this analysis, the combinations with steel fibers were taken as a reference, comparing their performance with the hybrid combinations. Regarding the steel mixtures, it can be seen that the combination with 30kg led to a much-reduced fracture energy compared with the 50kg of steel fibres dosage (see Figure 10a). Comparing both steel dosages, differences of orders of magnitude from 550 to 1575N/m were reported for the different deflections, representing percentages of 41% to 65% (laboratory beams), and 60% to 77% (shotcrete beams) higher in favor of the 50SF combination.

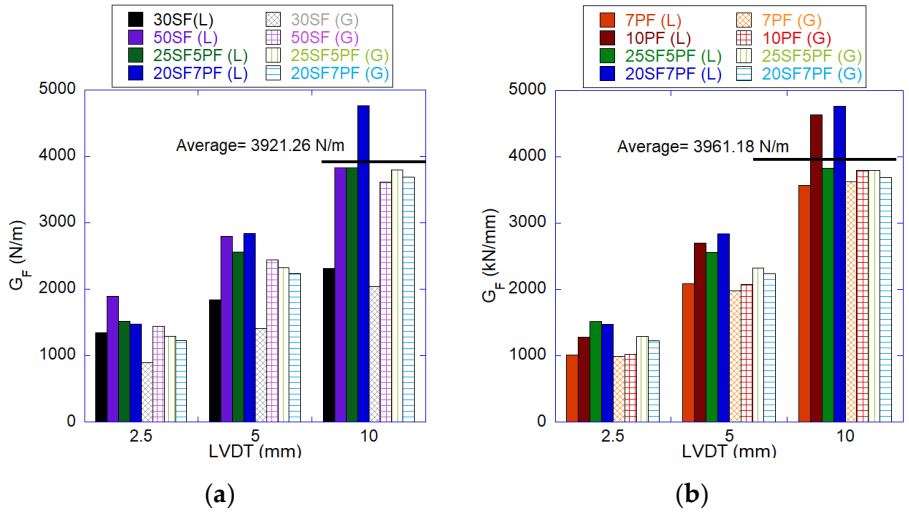

Figure 10. Fracture energy: (**a**) Steel and hybrid mixes; (**b**) Polyolefin and hybrid mixes.

Considering the dosages by weight, for the mixes with 30 kg/m^3 of fibers (30SF and 25SF5PF), the hybrid combination obtained a higher fracture energy on site and laboratory specimens. Evaluating the shotcrete specimens, the difference for a deflection of 2.5 mm was 44% in favor of the hybrid mix, increasing this value to 86% for a deflection of 10 mm.

Finally, analyzing both hybrid dosages in reference to the 50kg steel combination, all of them reported closer G_F values, especially for 5 and 10mm deflections, highlighting that for a 10mm deflection the hybrid samples 25SF5PF (G, L), and the sample 20SF7PF (L), reached a behavior equal and 24% higher than the sample 50SF(L), respectively.

3.3.3. Comparison between polyolefin and hybrid mixes

According to Figure 10b, the combination with 7 kg of polyolefins had a fracture energy lower than the rest of specimens, especially for ones tested in the laboratory, and for deflections smaller than 5 mm. Comparing the fracture energy of the mixtures with 7 and 10 kg/m^3 of polyolefins, the difference was in orders of magnitude: from 31 to 1067 N/m for the site and laboratory mixtures. Representing values from 3% to 5% (shotcrete beams), and 26% to 30% (laboratory beams) higher, in favor of the 10PF specimen. Considering only the fracture energies of the on situ specimens, it can be confirmed that both polyolefin mixtures obtained very similar values; the difference between their fracture energies for 5 and 10 mm was 89 N/m and 179 N/m, respectively. The influence of a higher volumetric fraction was not relevant for the performance on site.

Analyzing the fracture energy for a deformation of 10 mm, and considering the laboratory and on situ specimens, six of the eight beams obtained values between 3566 N/m to 3829 N/m, only the laboratory combinations 10PF and 20SF7PF exceeded these magnitudes, with values of 4634 N/m and 4766 N/m, respectively. The average value of these eight beams was 3961.18 N/m, slightly exceeding the average value of the steel and hybrid specimens represented in Figure 10a.

Preprints (www.preprints.org) | NOT PEER-REVIEWED | Posted: 3 June 2022 doi:10.20944/preprints202206.0037.v1

Finally, with respect to the shotcrete samples, it was confirmed that the polyolefin dosages had a slightly lower fracture energy (7PF), and similar (10PF) to the hybrid samples. In addition, the 10PF(L) mixture was able to obtain a very outstanding and even superior behavior, similar to the steel-polyolefin mixture 20SF7PF(L).

3.3.4. Residual strength, fracture energy and fiber count

This section presents a comparative analysis that relates residual strengths to fracture energy and includes the number of fibers counted in the fracture surface. According to the results commented in previous sections, the analysis is focused on the combinations with the best results: 50SF,10PF and both hybrid mixes. Figures 11 and 12 show these graphs classified according to fiber content.

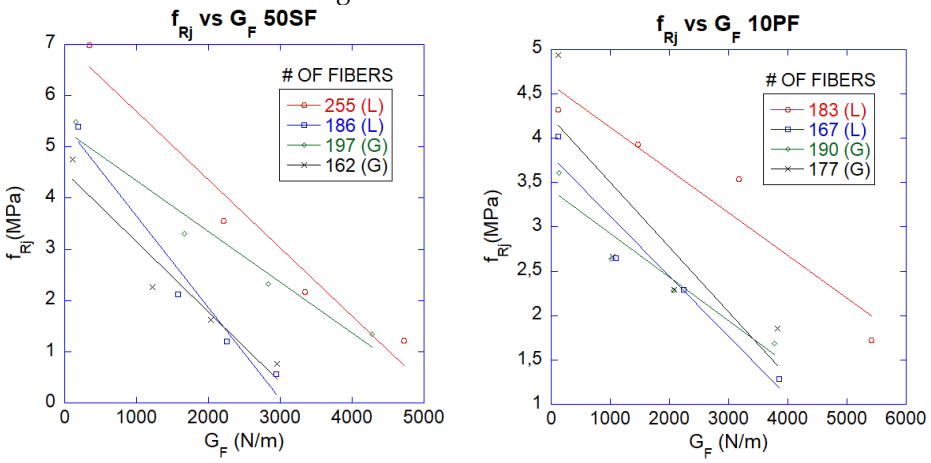

(**a**) (**b**)

Figure 11. Residual strength vs fracture energy: (**a**) 50SF; (**b**) 10PF.

- **50SF Y 10PF Mixes**

For the specimens with only steel fibres, it was evident that the higher the fiber content, the higher the residual strengths and fracture energies (Fig. 11a). It is worth noting that the combination with higher and lower fiber content 255(L) and 162(G) presented a parallelism, and this behavior could be attributed to a similar distribution of fibers in the fracture surface, but in different amounts. In addition, the combinations with 186(L) and 197(G) had an intersection in their peak load. The slope of the shotcrete specimen 197(G) was smaller, reporting a more controlled decrease of its f_{Rj} values with increasing fracture energy. On the contrary, 186(L) reported the opposite behavior, being the difference attributed to a lower percentage of fibers in the quadrants close to the notch.

Regarding the residual strength-energy fracture curves of the 10PF mix (Fig. 11b), it could be seen that the specimen with higher fiber content 190(G) obtained residual strengths even lower than specimens with lower number of fibers (167(L) and 177(G)), being this behavior was reported for a fracture energy up to 2000(N/m). Similarly, specimen 183(L) showed higher G_F and f_{Rj} values. Both mentioned behaviors are supported by the number of broken and slipped fibers in the fracture sections. Considering the average values of broken fibers in the fracture surface of the shotcrete (36 fibers) and laboratory specimens (66fibers), the difference was 83% in favor of the laboratory specimens. This dosage shows that a higher number of fibers does not guarantee a better performance of the concrete, being the failure form of the fibers and the anchorage of the fibers to the matrix were more relevant.

Finally, in most of the polyolefin mixes, the ratio of broken fibers to the total effective fibers in the fracture section represented 35%. That is to say, for percentages equal or higher than this, both f_{Rj} and G_F values were increased, having outstanding performance. The mentioned percentage was also present and valid in the specimens of hybrid combinations.

Preprints (www.preprints.org) | NOT PEER-REVIEWED | Posted: 3 June 2022 doi:10.20944/preprints202206.0037.v1

- **Hybrid mixes**

For these combinations the effect and influence of the number of broken fibers on the fracture section was significant. For example, for the 25SF5PF dosage (Fig. 12a), both laboratory mixtures obtained counts of 213 and 210 fibers, but only the latter reported the highest fracture energy and residual strength for strains greater than 5 mm. The specimen with 213 fibers exhibited even lower f_{Rj} and G_F values than the shotcrete combinations of 184 and 177 fibers, respectively. Considering the broken fiber count in the fractured section of the laboratory specimens, the 210(L) beam reported a 45% higher value.

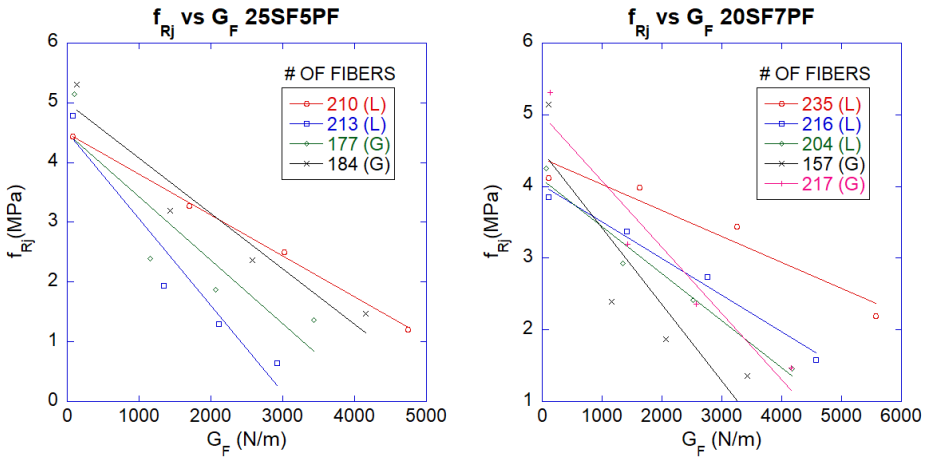

(**a**) (**b**)

Figure 12. Residual strength vs fracture energy: (**a**) 25SF5PF; (**b**) 20SF7PF.

Regarding the 20SF7PF combination (Fig. 12b), it can be distinguished that lineal regressions of the laboratory samples had a very similar slope, with more controlled decrease, and differentiated from the field specimens (157(G) and 217(G)) that exhibited more accentuated reduction. The lowest loss of residual strength and fracture energy was reported for the latter combinations. Comparing the average values of broken fibers, the laboratory beams reported twice the content (41 broken fibers), compared with the on site specimens (19 broken fibers). Again, the failure mode in the polyolefin fibers was responsible for the mechanical behavior and not the higher number of fibers in the section.

3.4. Plate test results

The results and classification of the tested plates according to their energy absorption capacity are presented below (see Table 3), delimited by the resistance classes established by EFNARC [28]. Likewise, the observed behavior was analyzed according to their load-deflection curves. All the combinations reached an energy absorption capacity equal to or higher than 700J for a deformation of 25 mm (Figure 13b). The combinations with lower fiber content (30SF and 7PF) reached a class B energy absorption capacity, while the rest of the mixtures reached class C. The mixture with 10 kg of polyolefin was the most outstanding, guaranteeing the application of this type of shotcrete for permanent support in hard soil, previously taking into consideration the characteristics of the rock mass, means of anchorage and soil subjection.

According to Fig. 13a, as well as the behavior reported for beams, the steel plate girders were able to withstand higher loads for initial deflections, reaching peak loads before 2 mm deflection, subsequently their load capacity decreased. In the case of polyolefin and hybrid mixtures, the peak load was obtained for deflections above 4 to 5 mm deflection, after which the load capacity decreased in a more controlled manner (see Figure 13a).

Preprints (www.preprints.org) | NOT PEER-REVIEWED | Posted: 3 June 2022 doi:10.20944/preprints202206.0037.v1

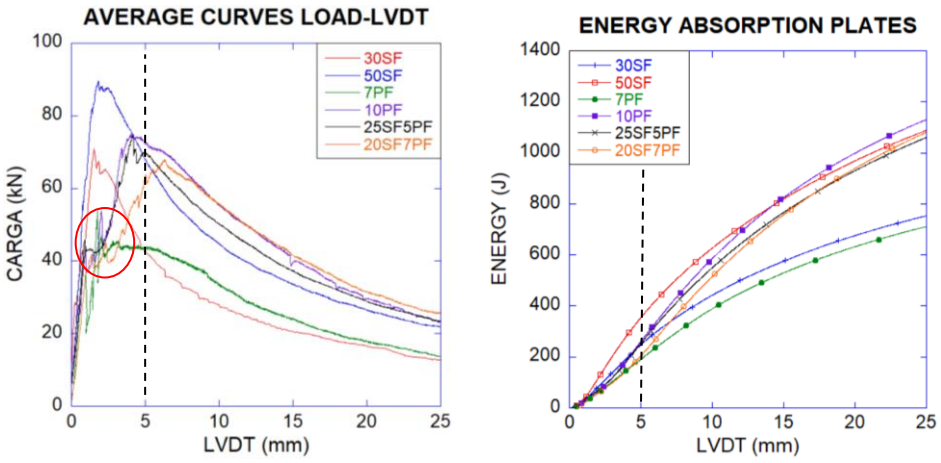

(**a**) (**b**)

Figure 13. Plate test curves: (**a**) Load-deflection; (**b**) Energy absorption-deflection.

This difference in load increase at different deformations can be attributed to the difference in adhesion and stiffness of the fibers, in this case the steel fibers being stiffer and having hooked ends, have a greater mechanical anchorage in the concrete [29-31], interacting from the beginning of the cracking of the concrete matrix, providing a higher initial load capacity. In the polyolefin-included and hybrid mixtures a load step was observed before reaching its maximum load (see Fig. 13a), delimited by a red circle. This behavior is attributed to the lower stiffness, and to the mechanism of working of polyolefins, that act gradually with the increase of the opening of the crack. They are able to withstand remaining loads higher than steel fibers [20], showing the combinations 10PF, 25SF5PF, 20SF7PF this behavior. Only the 7PF mix obtained a different behavior.

The analysis of the energy absorption capacity vs. deflection showed that the combinations with steel fibers were superior to the rest of the mixtures, up to 5 mm of deformation in the case of 30SF, and 10 mm for 50 SF (see Fig. 13b). This behavior was a product of the better mechanical anchorage and higher stiffness of the steel fibers, mentioned previously. The steel combinations were able to provide higher energy absorption E(J) at smaller deformations. For deformations larger than 5 and 10 mm, the hybrid and polyolefin blends performed better; only the 10PF combination was able to exceed the energy values achieved by the 50SF specimen.

3.4.1. Correlation of beam and plate tests

Initially, a comparative study was carried out about residual strengths vs. fracture energy in beams and plates. In the case of beams, the stress and fracture energy were obtained for deformations corresponding to the F_{LOP} load of 2.5, 5 and 10 mm. For plates, the points of the residual strength vs. fracture energy dispersion were determined for deflections equivalent to the F_{PEAK}, 2.5, 5, 10, 20, 25 and 30 mm. The stresses in plates were obtained based on the Mindlin-Reissner theory, and the fracture energy was determined considering the work (energy absorption) and the area of the cracked section of the plate in the testing process, Figure 14 and equations 3 and 4 describe the process of obtaining the fracture energy.

Preprints (www.preprints.org) | NOT PEER-REVIEWED | Posted: 3 June 2022 doi:10.20944/preprints202206.0037.v1

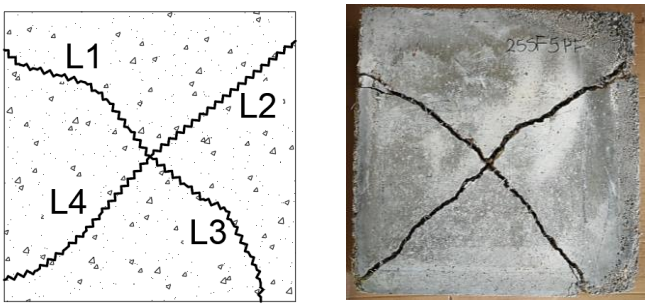

(**a**) (**b**)

Figure 14. Determination of cracking area.

$$A_{cracking} = l_1 \cdot h + l_2 \cdot h + \cdots + l_i \cdot h \quad (3)$$

l_i: crack length
h: plate height (10cm)

$$G_{F\,plates} = \frac{\int F\delta}{A_{cracking}} \quad (4)$$

Figure 15 presents the residual strength vs. fracture energy relationships for beams and plates, for the steel (50SF), polyolefin (10PF) and hybrid combinations. All the linear fits of the plates had a similar negative slope, but with a displacement on the vertical axis, much higher than the beams due to their higher load capacity during the testing process, and the parallelism of these fits was evident in all cases.

This behavior pattern allows to extrapolate the values from beams to plates and vice versa, being this approximation conditioned by the content and type of fiber analyzed. The extrapolation from beams to plates is valid for deformations in beams corresponding to f_{LOP}, up to 10 mm of deflection, since in the beam test we cannot reach the degree of deformation in plates (30 mm). It should be noted that in all cases the fracture energy was not the same in plates and beams for the same deformation, and they do not have a biunivocal G_F-deformation correspondence. This fracture energy is directly related to the content and distribution of fibers in the plate and to the multi-cracking process. Only the 10PF combination presented very close fracture energies in beams and plates for deformations of 2.5, 5 and 10 mm.

Therefore, by making approximations of f_{Rj}-G_F from beams to plates with the increments presented in Figure 15, it will allow obtaining indicative results. The increase of residual strength Δf_{Rj}, was in the range of 5.31 MPa to 6.34 MPa, considering the mixtures with higher content of polyolefin fibers and steel, and both hybrid mixtures. In addtion, considering the fracture energy for the highest deformations (10 mm in beams, and 30 mm in plates), the difference was 227% to 283% higher in the plate tests, product of the multiple cracking process that offers a higher energy absorption capacity and due to a larger fracture section.

Preprints (www.preprints.org) | NOT PEER-REVIEWED | Posted: 3 June 2022 doi:10.20944/preprints202206.0037.v1

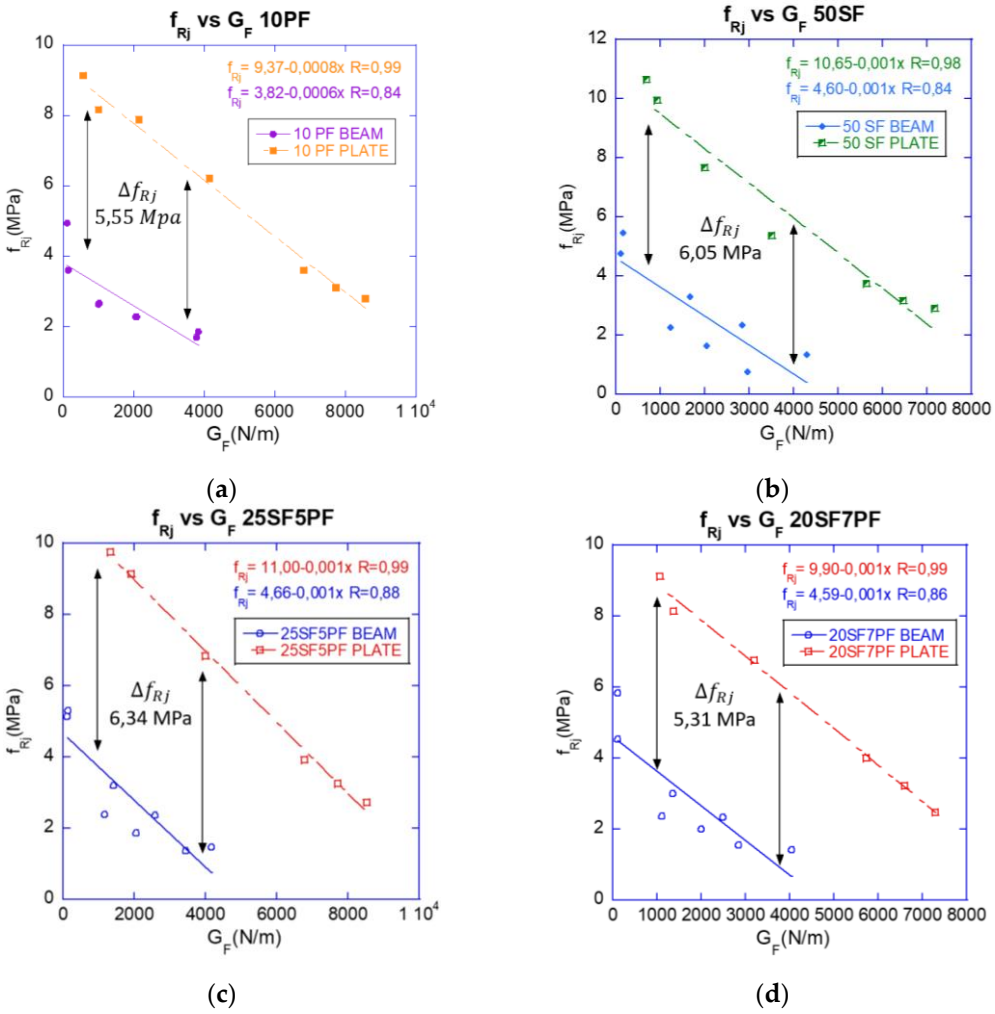

Figure 15. Residual strength vs fracture energy on plates and beams: (**a**) 10PF; (**b**) 50SF; (**c**) 25SF5PF; (**d**) 20SF7PF.

Figure 16 shows the correlation of residual resistances in beams for a deformation of 3 mm versus values of the energy absorption capacity for a deflection of 25 mm in plates, analysis also performed by Bernard [32]. This deformation of 3 mm in beams corresponded to a crack opening (CMOD) of 3.35 mm in most of the beams.

Finally, the residual tensile bending resistance for a deflection of 3 mm can be obtained by the equation f_{Rj} (in MPa) = 3-E25mm (Joules)/125 (r=0.87), this equation can also be used to find the energy absorption capacity. Giving approximate values that allow to consider and ratify values of energy absorption in slabs, being able to reformulate and make adjustments to the dosage of the analyzed fiber shotcrete.

Preprints (www.preprints.org) | NOT PEER-REVIEWED | Posted: 3 June 2022 doi:10.20944/preprints202206.0037.v1

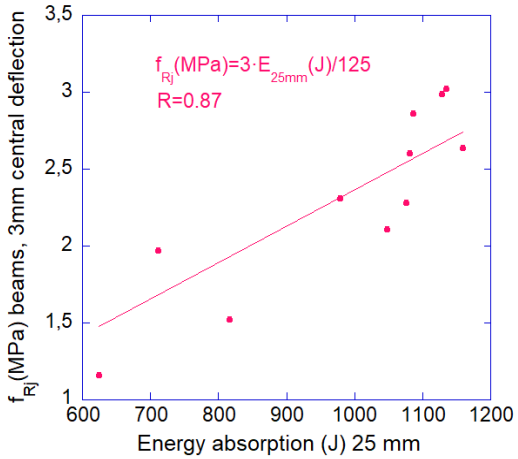

Figure 16. Residual strength in beams for 3mm deflection vs. energy absorption capacity in plates for 25mm deflection.

4. Conclusions

In all mixes, the residual flexural strengths for the shotcrete beams (G) were lower. This reduction was more appreciable in the steel fibre combinations, reporting losses of 73 to 11% for f_{R1} and f_{R3}, respectively, while the polyolefin and hybrid samples exhibited reductions of 20% to 10%.

The synergy of the hybrid combinations (steel-polyolefin) was notorious, highlighting that the higher the content of steel fibers, the higher the residual strengths for lower crack openings (CMOD= 2 mm). On the contrary, a higher polyolefin content achieved higher residual strengths for greater CMOD (2 mmto 6 mm) but lower initial residual strength (see Figure 5). Tthe combination with higher steel content, 25SF5PF, was the optimal.

The fiber content and orientation factor of the fractured assessed at the fracture surface was lower in the steel and hybrid shotcrete specimens, only the polyolefin mixtures reached higher values than laboratory. This behavior is attributed to a lower adhesion capacity of the steel fibers to the concrete matrix in the fresh state, compared with fibers of polymeric origin during shotcreting process [25-27].

For hybrid and polyolefin mixtures, a higher fiber content did not guarantee a better performance in fracture energy and residual strengths. The higher number of broken fibers and better anchorage to the matrix was relevant. Specimens with 35% broken fibers in the fracture surface as a proportion of total polyolefin fibers had superior performance.

The correlation of residual strengths and fracture energies between plates and beams showed a certain parallelism that allows to estimate approximate values in plates from beam tests considering the increment Δf_{Rj}. Similarly, the residual strength (f_{Rj}) for a deflection of 3 mm in beams versus E_{25mm} in slabs, allows to estimate valid approximations, helping to reformulate or make adjustments in the dosage of the fiber concrete analyzed.

Author Contributions: Conceptualization, A.B. and A.M.; methodology, A.B., C.A., A.M. and J.C.G.; software, A.B.; validation, A.B., C.A. and A.M.; formal analysis, A.B. and C.A.; investigation, A.B. and C.A.; resources, A.B. and C.A.; data curation, C.A.; writing—original draft preparation, A.B. and C.A.; writing—review and editing, A.B., C.A., A.M. and J.C.G.; visualization, A.M.; supervision, A.M. and J.C.G.; project administration, A.M. and J.C.G. All authors have read and agreed to the published version of the manuscript.

Funding: This research was funded by the Ministry of Science and Innovation of Spain by means of the Research Fund Project PID2019-108978RB-C31R.

Data Availability Statement: Not applicable.

Acknowledgments: In this section, you can acknowledge any support given which is not covered by the author contribution or funding sections. This may include administrative and technical support, or donations in kind (e.g., materials used for experiments).

Conflicts of Interest: The authors declare no conflict of interest

References

1. C. Leung, R. Lai and A. Lee, "Properties of wet-mixed fiber reinforced shotcrete and fiber reinforced concrete with similar composition". *Cement and Concrete Research* **2005**, *vol. 35*, *no. 4*, pp. 788-795.
2. D. Morgan, L. Chen and D. Beaupre, "Toughness of fiber reinforced shotcrete". *Shotcrete for Underground Support VII, ASCE* **1995** pp. 66-87.
3. M. Vandewalle, "*Tunnelling the World*". Bekaert S.A:Belgium, 1997.
4. Y. Potvin and P. Nedin, "Controlling rockfall risks in Australian underground metal mines". *Ground Support in Mining and Underground Construction* **2004**, pp. 359-366.
5. E. S. Bernard, "Safe support with fibre reinforced shotcrete" *Tunnel.J.* **(September) 2013**, pp. 44-47.
6. A. Lang and C. Stubley, "Rockfalls in Western Australian underground metalliferous mines". *Ground Support in Mining and Underground Construction* **2004**, pp. 375–386.
7. G. Hoff, "Durability of fiber reinforced concrete in a severe marine environment". *American Concrete Institute Special Publication* **1987**, no. 100, pp. 997-1042.
8. International Tunnelling Association, "Guidance For Precast Fibre Reinforced Concrete Segments - vol.1: Design aspects" *ITAtech Report* **April 2016**,*No. 7*.
9. J. Kaufmann, Durability performance of fiber reinforced shotcrete in aggressive environment. In Proceedings of World Tunnelling Congress p. 7,Foz do iguaçu,Brazil, May 2014.
10. E. Bernard, "2015b. Effect of exposure on post-crack performance of FRC for tunnel segments," Dubrovnik, 2015.
11. P. Mangat and K. Gurusamy, "Permissible crack widths in steel fibre reinforced marine concrete". *Materials and structures* **1987**, *vol. 20*, *no. 5*, pp. 338-347.
12. A. Thomas and R. Dimmock, "The design philosophy for permanent sprayed concrete linings – Surface challenges – Underground solutions". In Proceedings of World tunnel congress, Bergen, Norway, 2017.
13. B. Chen and J. Liu, "Contribution of hybrid fibers on the properties of the high-strength lightweight concrete having good workability". *Cement and Concrete Research* **2005**, *vol. 35*, *no. 5*, pp. 913-917.
14. P. Song, J. Wu, S. Hwang and B. Sheu, "Statistical analysis of impact strength and strength reliability of steel–polypropylene hybrid fiber-reinforced concrete". *Construction and building materials* **2005**, *vol. 19*, *no. 1*, pp. 1-9.
15. O. Cengiz and L. Turanli, "Comparative evaluation of steel mesh, steel fibre and high-performance polypropylene fibre reinforced shotcrete in panel test". *Cement and concrete research* **2004**, *vol. 34*, *no. 8*, pp. 1357-1364.
16. J. Yang, J. Kim and D. Yoo, "Performance of shotcrete containing amorphous fibers for tunnel applications". *Tunnelling and Underground Space Technology* **2017**, *vol. 64*, pp. 85-94.
17. F. Jeng, M. Lin and S. Yuan, "Performance of toughness indices for steel fiber reinforced shotcrete". *Tunnelling and underground Space technology* **2002**, *vol. 17*, *no. 1*, pp. 69-82.
18. EN 14651:2005+A1, Test Method for Metallic Fibre Concrete. Measuring the Flexural Tensile Strength (Limit of Proportionality LOP) Residual), 2007. Available online: https://www.en-standard.eu/bs-en-14651-2005-a1-2007-test-method-for-metallic-fibre-concrete-measuring-the-flexural-tensile-strength-limit-of-proportionality-lop-residual/ (accessed on 23 April 2022)
19. B. Barr, M. Lee, E. de Place Hansen, D. Dupont, E. Erdem, S. Schaerlaekens, B. Schnütgen, H. Stang and L. Vandewalle, "Round-robin analysis of the RILEM TC 162-TDF beam-bending test: Part 3—Fibre distribution" *Materials and Structures* **2003**, *vol. 36*, *no. 9*, pp. 631-635.
20. M. G. Alberti. Polyolefin fibre-reinforced concrete: from material behaviour to numerical and design considerations-Tesis Doctoral, Madrid: Universidad Politécnica de Madrid,E.T.S. de Ingenieros de Caminos,Canales y Puertos, 2015.
21. AENOR. *UNE-EN 14488-1:2006 Ensayos de hormigón proyectado. Parte 1: Toma de muestras de hormigón fresco y endurecido*, Madrid-España: Asociación Española de Normalización y Certificación, 2006.
22. AENOR. UNE-EN 14488-5:2007 Ensayos de hormigón proyectado. Parte 5: Determinación de la capacidad de absorción de energía de probetas planas reforzadas con fibras, Madrid-España: Asociación Española de Normalización y Certificación, 2007.
23. Borrador Código Estructural, CE-18, Madrid: Secretaría General Técnica Ministerio de Fomento, 2018.
24. L. Malmgren. "Strength, ductility and stiffness of fibre-reinforced shotcrete". *Magazine of Concrete Research* **2007**, *vol. 59*, *no. 4*, pp. 287-296.
25. J. Kaufmann, K. Frech, P. Schuetz and B. Münch. "Rebound and orientation of fibers in wet sprayed concrete applications" *Construction and Building Materials* **2013**, *vol. 49*, pp. 15-22.
26. H. Armelin. Rebound and toughening mechanisms in steel fiber reinforced dry-mix shotcrete,Doctoral dissertation, Vancouver, BC, Canada: University of British Columbia, 1997.
27. S. Austin, C. Peaston and P. Robins. "Material and fibre losses with fibre reinforced sprayed concrete". *Construction and Building Materials* **1997**, *vol. 11*, *no. 5-6*, pp. 291-298.
28. EFNARC, "European specification for sprayed concrete," 1996.

 doi:10.20944/preprints202206.0037.v1

29. F. Isla, G. Ruano and B. Luccioni. "Analysis of steel fibers pull-out. Experimental study". *Construction and Building Materials* **2015**, *vol. 100*, pp. 183-193.
30. M. Tuyan and H. Yazıcı. "Pull-out behavior of single steel fiber from SIFCON matrix". *Construction and Building Materials* **2012**, *vol. 35*, pp. 571-577.
31. F. Laranjeira, C. Molins and A. Aguado. "Predicting the pullout response of inclined hooked steel fibers". *Cement and concrete research* **2010**, *vol. 40*, *no. 10*, pp. 1471-1487.
32. E. Bernard. "Correlations in the behaviour of fibre reinforced shotcrete beam and panel specimens," *Materials and Structures* **2002**, *vol. 35*, *no. 3*, pp. 156-164.
33. American Concrete Institute, ACI 506R-16 Guide to Shotcrete, Farmington Hill,MI: American Concrete Institute, 2016, p. 56.
34. V. P. Villar. Implicaciones de la alineación predecible de fibras metálicas mediante campos magnéticos en materiales cementosos para el diseño y construcción de estructuras superficiales (Tesis doctoral), Madrid: Universidad Politécnica de Madrid, 2017.
35. International Tunneling Association. *Shotcrete for Rock Support Guidelines and Recommendations*, Stockholm: Swedish Rock Engineering Research Foundation, 1993.
36. C. Leung, R. Lai and A. Lee. "Properties of wet-mixed fiber reinforced shotcrete and fiber reinforced concrete with similar composition". *Cement and Concrete Research* **2005**, *vol. 35*, *no. 4*, pp. 788-795.
37. Instrucción del Hormigón Estructural, EHE-08, Madrid: Ministerio de Fomento, Secretaría General Técnica, 2008
38. P. S. Song and S. Hwang. "Mechanical properties of high-strength steel fiber-reinforced concrete". *Construction and Building Materials* **2004**, *vol. 18*, *no. 9*, pp. 669-673.
39. S. Kang and J. Kim. "The relation between fiber orientation and tensile behavior in an Ultra High Performance Fiber Reinforced Cementitious Composites (UHPFRCC)". *Cement and Concrete Research* **2011**, *vol. 41*, *no. 10*, pp. 1001-1014.
40. P. Soroushian and C. Lee. "Distribution and orientation of fibers in steel fiber reinforced concrete". *Materials Journal* **1990**, *vol. 87*, *no. 5*, pp. 433-439.
41. M. Di Prisco, M. Colombo and D. Dozio. "Fibre-reinforced concrete in fib Model Code 2010: principles, models and test validation". *Structural Concrete* **2013**, *vol. 14*, *no. 4*, pp. 342-361.
42. M. Alberti, A. Enfedaque and J. Gálvez. "On the mechanical properties and fracture behavior of polyolefin fiber-reinforced self-compacting concrete". *Construction and Building Materials* **2014**, *vol. 55*, pp. 274-288.
43. D. Dupont and L. Vandewalle. "Distribution of steel fibres in rectangular sections". *Cement and Concrete Composites* **2005**, *vol. 27*, *no. 3*, pp. 391-398.